

Contents lists available at ScienceDirect

Analytica Chimica Acta

journal homepage: www.elsevier.com/locate/aca



Speciation of thioarsenicals through application of coffee ring effect on gold nanofilm and surface-enhanced Raman spectroscopy



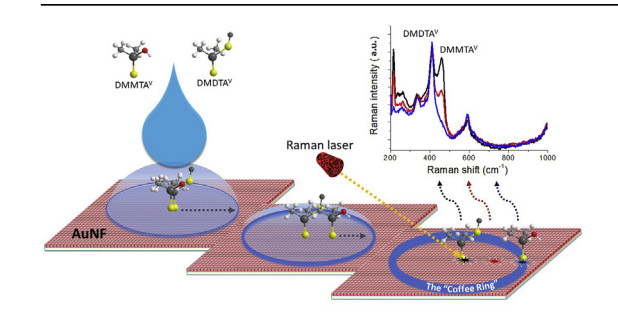
Valery Liamtsau ^a, Changjun Fan ^a, Guangliang Liu ^a, Anthony J. McGoron ^b, Yong Cai ^{a, c, *}

- ^a Department of Chemistry and Biochemistry, Florida International University, Miami, 11200 SW 8th ST, Miami, FL, 33199, USA
- ^b Biomedical Engineering Department, Florida International University, 10555 West Flagler Street, EC 2442, Miami, FL, 33174, USA
- ^c Southwest Environmental Research Center, Florida International University, 11200 SW 8th ST, Miami, FL, 33199, USA

HIGHLIGHTS

- Gold nanofilm (AuNF)-based coffee ring effect combined with SERS for analysis of thioarsenicals.
- Manipulating conditions based on chemical properties of thioarsenicals for better separation.
- · Demonstration of coupling coffee ring effect separation to SERS detection for small molecules.

G R A P H I C A L A B S T R A C T



ARTICLE INFO

Article history: Received 2 October 2019 Received in revised form 15 January 2020 Accepted 18 January 2020 Available online 21 January 2020

Keywords: Coffee ring effect Gold nanofilm Surface-enhanced Raman spectroscopy Thioarsenicals

ABSTRACT

Thioarsenicals, such as dimethylmonothioarsinic acid (DMMTAV) and dimethyldithioarsinic acid (DMDTA^V), have been increasingly discovered as important arsenic metabolites, yet analysis of these unstable arsenic species remains a challenging task. A method based on surface-enhanced Raman spectroscopy (SERS) detection in combination with the coffee ringeffect for separation is expected to be particularly useful for analysis of thioarsenicals, thanks to minimal sample pretreatment and unique fingerprint Raman identification. Such a method would offer an alternative approach that overcomes limitations of conventional arsenic speciation techniques based on high performance liquid chromatography separation and mass spectrometry detection. A novel analytical method based on combination of the coffee ringeffect and SERS was developed for the speciation of thiolated arsenicals. A gold nanofilm (AuNF) was employed not only as a SERS substrate, but also as a platform for the separation of thioarsenicals. Once a drop of the thioarsenicals solution was placed onto the AuNF and evaporation of the solvent and the ring stamp formation onto AuNF began, the SERS signal intensity substantially increased from center to edge regions of the evaporated droplet due to the presence of the coffee ring effect. Through calculating the pKa's of DMMTAV and DMDTAV and accordingly manipulating the chemical environment, separation of these thioarsenicals was realized as they travelled different distances during the development of the coffee ring. The migration distances of individual species were influenced by a radial outward flow of a solute, the thioarsenicals-AuNF interactions and a thermally induced Marangoni flow. The separation of DMMTAV (center) and DMDTAV (edge) on the coffee ring, in combination with fingerprint SERS spectra, enables the identification of these thioarsenicals by this AuNF-based coffee ring effect-SERS method.

© 2020 Elsevier B.V. All rights reserved.

Corresponding author. Department of Chemistry and Biochemistry, Florida International University, Miami, 11200 SW 8th ST, Miami, FL, 33199, USA. E-mail address: cai@fin edu (Y Cai)

1. Introduction

Thioarsenicals, which contain an arsenic—sulfur bond analogous to their oxoarsenical counterpart with an arsenic—oxygen bond, have been increasingly discovered as a new class of arsenic metabolites in recent years [1—3]. Dimethylmonothioarsinic acid (DMMTA^V) and dimethyldithioarsinic acid (DMDTA^V) were widely detected in animal urine after exposure to various arsenic compounds, including dimethylarsinic acid (DMA^V) (Fig. 1) [4]. Dimethylarsinothioyl glutathione (DMMTA^V(GS)), a conjugate of pentavalent arsenical DMMTA^V with glutathione (GSH), has been detected in cabbage (Brassica oleracea) after exposure to DMA^V and in human cell lines exposed to darinaparsin [5,6]. After introduction of DMA^V to Shewanella putrefaciens, DMMTA^V has been observed during arsenic biotransformation [7].

The generation of pentavalent thioarsenicals during As metabolism is of particular interest due to their ability to bind to the proteins in contrast to their oxygenated analogues. According to the Pearson's hard/soft acid—base (HSAB) concept, pentavalent oxygenated As species are not likely to complex with proteins via interacting with thiol groups of peptides such as glutathione (GSH) and metallothioneins [5]. However, sulfur in thioarsenicals mitigates the hardiness of a molecule making it possible to bind to the proteins, possibly leading to higher toxicity. Previous toxicity tests confirmed that the toxicities of pentavalent thioarsenicals are similar with that of trivalent inorganic species (iAs^{III}) and are much higher than those of pentavalent oxygen-containing analogues, e.g., DMA^V [8]. For instance, DMMTA^V can bound to rat hemoglobin, illustrating that pentavalent As interacts with —SH groups of proteins and peptides [9].

Thioarsenicals appear to be among the key intermediates involved in arsenic metabolism due to their wide detection of in biological samples post As exposure, capability of binding to proteins, and potentially high toxicity. Accurate speciation analysis of thioarsenicals has increasingly become demanding, albeit challenging. The speciation of thioarsenicals has been usually performed by high-performance liquid chromatography (HPLC) coupled with inductively coupled plasma mass spectrometry (ICP-MS) and/or electrospray ionization mass spectrometry (ESI-MS) methods [10-13]. However, there are some drawbacks associated with these conventional HPLC-ICP-MS or ESI-MS methods for analysis of thioarsenicals. First, thioarsenicals are unstable species, and they could be decomposed at acidic pH and/or in the presence of oxygen during the extraction from biological samples [14–18]. Second, species alteration may occur during the analysis, as observed in HPLC separation of thio-organoarsenate (2dimethylarsinothioyl acetic acid), where the acidic mobile phase degrades the analyte momentarily, while weak acidic solution makes it almost impossible to elute the analyte from the column [18]. Another problem of these conventional methods is the lack of precise structural information, as exemplified by the misidentification of DMMTA^V as DMA^{III} due to similar chromatographic properties [1]. Similarly, in the study of pentavalent thioarsenicals complexed with GSH, it is not conclusive from analyzing the ESI-MS data whether the thioarsenical is pentavalent (GSH directly bound

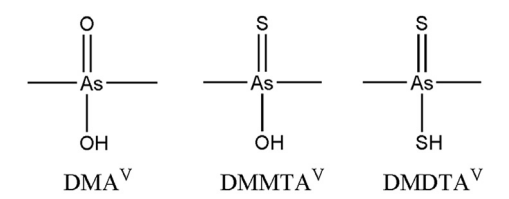


Fig. 1. Thioarsenicals analogous to the oxoarsenical counterpart.

to As through its cysteine unit) or trivalent (GSH bound through a sulfur—sulfur bridge to As) [5].

Due to the drawbacks of currently available methods for analysis of thioarsenicals, it is believed that the inaccurate information (e.g., underestimation and/or speciation conversion) was associated with analysis of thioarsenicals in previous studies. There is a need for a method that can provide researchers with detailed structural information and does not require extensive sample preparation for accurate analysis of thioarsenicals. We reason that a method based on surface-enhanced Raman spectroscopy (SERS) detection in combination with the coffee ring effect for separation could be particularly useful for analysis of unstable thioarsenicals thanks to minimal sample pretreatment and unique fingerprint Ramon identification. A coffee ring deposit forms through evaporation of solvent when a drop of liquid is placed on the solid surface [19]. The coffee ring effect has found its way in analytical applications, for separation of particles and large biomolecules exploiting the size difference of analytes. Methods based on coupling the coffee ring effect with matrix-assisted laser desorption (MALDI) and Raman spectroscopy [20] were successfully applied for the separation and identification of differentsized particles [21], polymer-nanocrystal mixtures [22] and polycyclic aromatic hydrocarbons [23].

We previously applied SERS coupled with the coffee ring effect on silver nanofilms (AgNFs) to speciate arsenite (As^{III}), arsenate (AsV), monomethylarsonic acid (MMAV) and dimethylarsinic acid (DMAV), four common, relatively stable arsenic species [24]. It is more important to apply SERS-based methods to analysis of thioarsenicals, as they are unstable and could decompose when using conventional HPLC separation [18] and ESI-MS detection [5], which might be of the reasons why they have been detected only in recent years. We propose here to develop a more robust nanomaterials-based SERS analytical method for detection of thioarsenicals, by considering the interactions of As species with the substrate surface and manipulating the coffee ring effect to facilitate the separation of thioarsenicals. As the information on basic physicochemical properties of these compounds remains lacking, we calculated the pKa values of DMMTAV and DMDTAV and selectively adjusted pH in a way that DMMTAV and DMDTAV carried different charges and thus interacted differently with the surface during coffee ringformation for better separation. Although we previously reported the Raman spectra of some of thioarsenicals [25], we adjusted the theoretical calculations to the changing pH environment, considering that acidic or basic pH could considerably influence the Raman spectra of DMDTAV. We used a gold nanofilm (AuNF) as the SERS substrate, not only to enhance an inherently wear Raman signal [26,27], but also to avoid oxidation of thioarsenicals. Combining signature Raman spectra due to distinct chemical structures and properties and different migration distances of DMMTAV and DMDTAV in the coffee ring stain, we successfully differentiated these two thioarsenicals on AuNFbased SERS.

2. Experimental

2.1. Materials and chemicals

Cacodylic acid sodium salt, 98% (DMA^V), NaOH, HCl, Citric acid, Sodium citrate dihydrate (Granular certified), (3-Aminopropyl)trimethoxysilane (APTMS), glass microscope slides, weighing boats and 25 ml glass vials were purchased from Fisher scientific Inc (Hampton, NH). The citrate buffer (pH = 3) was fabricated by mixing Citric acid and Sodium citrate. All solutions were prepared in deionized (DI) water (18.2 M Ω , Barnstead Nanopure Diamond).

2.2. Instrumentation

The Raman spectrometer was obtained from PerkinElmer (Raman station 400F), which employed a diode laser at 785 nm with an average power of 100 mW. An infrared (IR) laser is used here, implying that the application of IR measurement is possible for these thioarsenicals. For instance, surface enhanced infrared absorption spectroscopy (SEIRAS) could be employed for the intensification of IR active vibrational modes, providing additional information regarding the thioarsenicals' vibrational frequencies that may be Raman inactive and thus more complete structural vibrational information on these arsenicals [28]. This Raman station was equipped with one PerkinElmer microscopy 300 with portable stage and a camera to observe the sample surface. For optimizing resolving power, the 20 \times optical lens focusing was acquired. A silicon wafer was employed to calibrate the Raman system at a daily use and the Raman signal intensity at 522 cm⁻¹ was monitored to check the reproducibility of the instrument. The SERS measurement parameters were laser wavelength, 785 nm; exposure time, 1 s; and 4 times of exposure per measurement. The AuNF surface was characterized by the Veeco multimode atomic force microscope (AFM), Malvern Zetasizer Nano-ZS (Westborough, MA) was employed for the measurements of nanoparticles size (average diameter) and zeta potential. All pH measurements were carried out on a Fisher Scientific Research AR15 pH/mV/°C Meter.

2.3. Synthesis of thioarsenicals and determination of their respective Raman spectra

2.3.1. Dimethylmonothioarsenious acid (DMMTA^V)

DMMTA^V was synthesized according to the method reported by Cullen et al. [29] (Fig. 2A). Briefly, DMA^V (2.76 g) and sodium Na₂S * 9H₂O (7.60 g) were dissolved in 30 mL of water. Concentrated H₂SO₄ (1.70 mL) was added dropwise to the solution to make molar ratio of Na₂S/H₂SO₄/DMA^V was 1.6:1.6:1. The reaction mixture was stirred for 1 h and was extracted with ether and was dried over anhydrous Na₂SO₄. The ether was evaporated under N₂ and colorless crystals were formed. Raman spectra determined of both solid and liquid forms (citrate buffer solution, pH = 3) of DMMTA^V were identical.

2.3.2. Dimethyldithioarsenious acid (DMDTA^V)

DMDTA^V was synthesized by two different methods. The first method for DMDTA^V synthesis was reported by Suzuki et al. [30] (Fig. 2B). Briefly, cacodylic acid (1.01 g) and Na₂S*9H₂O (4.27 g)

A)
$$\longrightarrow$$
 As OH \longrightarrow Na₂S, H₂SO₄ \longrightarrow As OH DMMTAV

B) \longrightarrow As OH \longrightarrow Na₂S, H₂SO₄ \longrightarrow As SH DMAV

C) \longrightarrow As OH \longrightarrow CDMAV DMDTAV

 \longrightarrow Na

 \longrightarrow Na

Fig. 2. Synthesis reactions of A) DMMTA V , B) DMDTA V (acid form), and C) DMDTA V (salt form) from DMA V .

were dissolved in water (15 ml) and concentrated H_2SO_4 (2.90 ml) was added. The molar ratio between components $Na_2S/H_2SO_4/DMA^V$ was 7.5:7.5:1. The mixture was stirred for 3 h, then DMDTAV was extracted with ether and was dried over anhydrous Na_2SO_4 . After ether evaporation under N_2 and colorless crystals were formed. Raman spectra determined of both solid and liquid forms (citrate buffer solution, pH=3) of DMDTAV were not identical, once a solid was dissolved into the citrate buffer, it formed a salt form that had a different vibrational fingerprint of As—S vibrations.

The second approach was reported by Fricke et al. [31] (Fig. 2C). Briefly, cacodylic acid (1.01 g) and NaOH (0.29 g) were dissolved in boiling ethanol (12.5 mL). Hydrogen sulfide was bubbled into the boiling solution for 30 min, and a white solid precipitated. After cooling, colorless crystals were isolated by filtration and air dried. Raman spectra determined of both solid and liquid forms (citrate buffer solution, pH = 3) of DMDTA V (salt form) were identical.

2.4. Theoretical calculation of Raman spectra of DMMTA V and DMDTA V

The theoretical calculation was completed employing Gaussian 09 in Florida International University's HPC facility. Firstly, MOL-DEN visualization software [32] creates and optimizes the unique molecular vibrations for specific bonds at certain vibrational frequencies; Secondly, Multiwfn translates Raman signals from the data acquired from Gaussian output into Raman intensities, thus creating the simulated Raman graph for thioarsenicals [33]. Density functional theory (DFT) derived Raman spectra was measured by MOLDEN molecular simulation, while assignments from crystal Raman spectra were employed to verify MOLDEN assignments [34]. The results obtained with a hybrid functional B3LYP approach using the basis set $6-311++G^{**}$ were proven by our research group [25] as a method that provides computational efficiency and precision in vibrational frequency prediction for computational spectra of oxygenated arsenicals, resulting in the lowest RMS value among other calculation methods tested. The Chem 3D optimized structures of DMMTA^V, DMDTA^V acid and salt forms are shown in Fig. S1. The comparison between the DFT calculated and experimental Raman spectra of thioarsenicals is summarized in Table S1.

2.4.1. Calculations of pKa's values for DMMTA^V and DMDTA^V

The pKa's values of these thioarsenicals are important factors in determining their behavior on the AuNF surface. If DMMTAV and DMDTAV would have pKa's that substantially differ from each other, it could be sensible to selectively deprotonate one of the thioarsenicals, leaving another uncharged. Depending on the differences in pKa's values of DMMTAV and DMDTAV, buffers will be used to manipulate the charges of thioarsenicals, making them have different charges. There were no reports with regards to their pKa's values [35], therefore computational program was employed for the pKa's calculation. Marvin Sketch version 17.14 (ChemAxon Kft) was proven to perform reliable pKa's calculation based on molecular structure of species [36,37]. For example, calculated by this software pKa's of ibuprofen [38], ynamines [39], and CH-acids were in agreement with literature value. Calculated pKa's value of inorganic pentavalent arsenic and methylated oxoarsenicals were consistent with the literature data [40,41], as shown in Table 1. This program was employed to calculate pKa's values of the thiolated arsenicals.

2.5. Fabrication of AuNF and application of the coffee ring effect for individual identification of DMMTA V and DMDTA V

The preparation of AuNF includes the synthesis of citrate-coated gold nanoparticles (AuNPs) and coating gold nanoparticles onto

Table 1 pKa's of arsenicals calculated by Marvin Sketch.

Arsenical	Literature data	Calculated in this work
MMA^V	$pKa_1 = 4.10$; $pKa_2 = 8.07$	$pKa_1 = 4.20$; $pKa_2 = 8.58$
DMA^V	pKa = 6.20	pKa = 6.22
DMMTA ^V	unknown	pKa = 4.37
DMDTA ^V	unknown	pKa = 2.25

glass slides. AuNPs were fabricated by reduction of chloroauric acid (HAuCl₄) with sodium citrate [42]. Briefly, the glassware was cleaned with Aqua Regia solution (HCl/HNO₃ = 3:1) overnight, then rinsed with DI water, followed by drying in an oven at 100 °C. After heating 20 ml of 1 \times 10⁻³ M HAuCl₄ chloroauric solution up to boiling point, sodium citrate (1 ml, 1%(v/v)) was introduced dropwise to this solution, and then refluxed for 30 min, following the production of red AuNPs colloidal suspension. The average size and zeta potential of AuNPs were 20 nm and -45 mV, respectively.

The fabrication of AuNF was performed by the silanization of the glass substrates, followed by the deposition of nanoparticles onto the silanized surface. AuNF was prepared according to the literature [43] with a slight modification of increasing the immersion time to 24 h. AuNF was characterized by AFM (Fig. S2, See supporting information).

DMMTA^V and DMDTA^V solutions 100 ppm solutions of thioarsenicals were prepared by dissolving thioarsenicals in citrate buffer (pH=3). Immediately after preparation 2 μ L of DMMTA^V and DMDTA^V citrate buffer solution were deposited onto AuNF. Once the droplet was completely dried and a ring-shaped stain was formed on the AuNF, SERS signals were measured from center to edge regions of the ring stain.

3. Results

3.1. Comparison of experimental and theoretically calculated Raman spectra of $DMMTA^V$ and $DMDTA^V$

DMMTA^V (solid/liquid form) Raman spectra exhibits three major vibrational modes observed at 469 cm⁻¹, 611 cm⁻¹ and 643 cm⁻¹. These represent As=S stretch, asymmetric vibrational mode of C-As-C and the As-O stretch, respectively [44] (Fig. 3A). The DFT

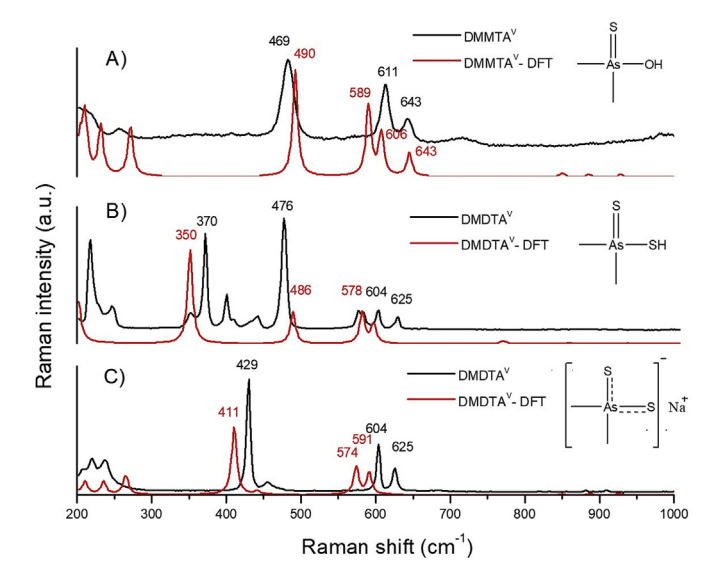


Fig. 3. Raman spectra (experimental and theoretical) of A) DMMTA^V, B) DMDTA^V (acid form) and C) DMDTA^V (salt form).

spectra of DMMTA^V showed the corresponding vibrations at 490 cm⁻¹, 606 cm⁻¹ and 643 cm⁻¹. In contrast to the theoretical Raman spectra of DMMTA^V, the symmetric vibrational mode of C–As–C (589 cm⁻¹) did not appear in the experimental Raman spectra possible because of the overlap with the C–As–C asymmetric vibration [25].

DMDTA^V in acid form (solid/liquid form) was synthesized by Method #1 [30], showing two major bands (Fig. 3B) represented by As–S stretch at 370 cm⁻¹ and As–S stretching at 475 cm⁻¹ [45]. Other vibrations are associated with the C–As–C symmetric mode (573, 604 cm⁻¹) and C–As–C asymmetric mode (625 cm⁻¹) respectively [46]. In contrast to DFT spectra of DMDTA^V, the symmetric mode of As–C stretching (578 cm⁻¹) was detected in crystalline form of DMDTA^V. Further considering the experimental spectra of DMDTA^V, the unknown Raman peak appeared in the region from 390 cm⁻¹ to 400 cm⁻¹, which might be originated from impurities. Also, the minor peak at 429 cm⁻¹ could be associated with the salt form of DMDTA^V (the synthesis byproduct) as elaborated in next paragraph.

The Raman spectra of DMDTAV(salt form), synthesized using Method #2 [31] (Fig. 3C) shows three major arsenic vibrational bands at 429 cm⁻¹, 604 cm⁻¹ and 625 cm⁻¹ related to As÷S vibration, C-As-C symmetric and asymmetric stretching. Comparing the Raman spectra of DMDTAV synthesized by two different methods, the As-S and As=S stretching of DMDTAV synthesized by Method #1 were observed, in contrast to only one As÷S (429 cm⁻¹) band represented by delocalized distribution π -electron cloud over S-As-S fragment in dimethyldithioarsinato anion [45,47], obtained by the Method #2. The bands at 604 cm⁻¹ and 625 cm⁻¹ represented symmetric and asymmetric C-As-C vibrations, respectively [44]. Notably, after addition of the NaOH to the acidic from of DMDTAV, the salt form occurred. Following this neutralization reaction, vibrational modes of As-S (370 cm⁻¹) and As=S (476 cm⁻¹) bands in acidic form of DMDTA^V merged into the delocalized π -electrons bond in salt form of DMDTA^V having the main signal at 429 cm⁻¹. The salt form of DMDTA^V is readily soluble in water in comparison to the acidic DMDTA^V [45]. All error ratios between experimental and theoretically calculated Raman frequencies were within 10%.

3.2. Identification of individual DMMTA^V and DMDTA^V using AuNF-

SERS spectra of DMDTAV and DMMTAV were obtained onto AuNF. Firstly, SERS spectra of thioarsenicals were acquired in the standard conditions (in the absence of the coffee ring effect). It is widely known that the coffee ring effect would be suppressed by the addition of the surfactants or organic solvents that decrease the droplet surface tension [48-50]. This reverses the radial outward flow and contributes to the even distribution of analytes across the coffee ring stain. The sodium dodecyl sulfate (SDS, 0.1%) was employed to alter the formation of the coffee ring deposit [51,52]. The differences between the Raman spectra of DMMTAV (solid/ liquid) and SERS spectra of DMMTAV (adsorbed onto AuNF, SDS) were observed during SERS measurements. Indeed, the wavelength red shift occurred for all DMMTAV vibrational frequencies, namely: from 469 cm $^{-1}$ to 464 cm $^{-1}$ for the As=S stretching, from 611 cm $^{-1}$ and 643 cm $^{-1}$ to 594 cm $^{-1}$ for the As=C symmetrical and asymmetrical stretching's respectively (Fig. 4A) [53]. The probable reason for this is the partial adsorption of DMMTA^V onto the AuNF surface, following a charge transfer effect between the AuNF surface and DMMTA^V. The most intense SERS signal of As=S vibration at 464 cm⁻¹ has been chosen for the tracing DMMTA^V across the coffee ring deposit. During the formation of the coffee ring stain (in the absence of SDS) the As=S stretching SERS intensity increased

from center to middle regions, however, despite the coffee ring effect, the decrease in SERS signal occurred in the edge region. Similar with the DMMTA^V, Raman spectra of DMDTA^V (solid/liquid) varies greatly from the SERS spectra of DMDTA^V (AuNF, SDS). Due to the charge transfer effect all DMDTA^V shifted to the red region: from 429 cm $^{-1}$ to 410 cm $^{-1}$ for π -delocalized S–As–S stretching, from 604 cm $^{-1}$ and 625 cm $^{-1}$ to 591 cm $^{-1}$ for As–C symmetric and asymmetric stretching respectively (Fig. 4B). A typical coffee ring phenomenon (increase of SERS intensity from center to edge regions) was observed for DMDTA^V deposition onto AuNF surface (in the absence of SDS). Indeed, the SERS signal of S–As–S stretching at 410 cm $^{-1}$ increases from the center to the edge region. Overall, the significant discrepancies between the SERS spectra of thioarsenicals in the presence/absence of the coffee ring effect were not observed.

Further to investigate the binding capacity of thioarsenicals onto AuNF surface, the SERS enhancement factors (EFs) of the corresponding thioarsenicals were calculated at pH=3 [27]. The extended calculations can be found in Fig. S4. The results showed that the EF for DMMTA^V (2.4×10^2) is slightly lower than that of DMDTA^V's EF (3.3×10^2) , which might be explained by the higher affinity of DMDTA^V to the AuNF surface. According to Fig. 4, the Raman shift of the As÷S stretching of DMDTAV (19 cm⁻¹) was significantly higher than that of DMMTAV (5 cm⁻¹), which corresponds to the different magnitude of the charge transfer between the individual thioarsenicals and the AuNF. At pH=3 DMDTAV molecule bears the negative charge, whereas DMMTAV is mostly neutral. This results in the different magnitude of the charge transfer and, consequently, Raman shift, Indeed, the negatively charged DMDTAV was adsorbed stronger onto the AuNF surface than DMMTA^V. Another factor that may govern the thioarsenicals-AuNF interactions is the amount of sulfur atoms in thioarsenicals molecules. DMDTAV having delocalized electron pair across S-As-S region lead to the stronger binding to AuNF in contrast to DMMTA^V that can be adsorbed through O–As=S moiety. Assuming the homogeneous coverage of AuNPs onto the AuNF surface, the electromagnetic part of enhancement affected the EF factors for both thioarsenicals in the similar way leaving the difference between the thioarsenicals EFs for the different chemical enhancement contribution [54].

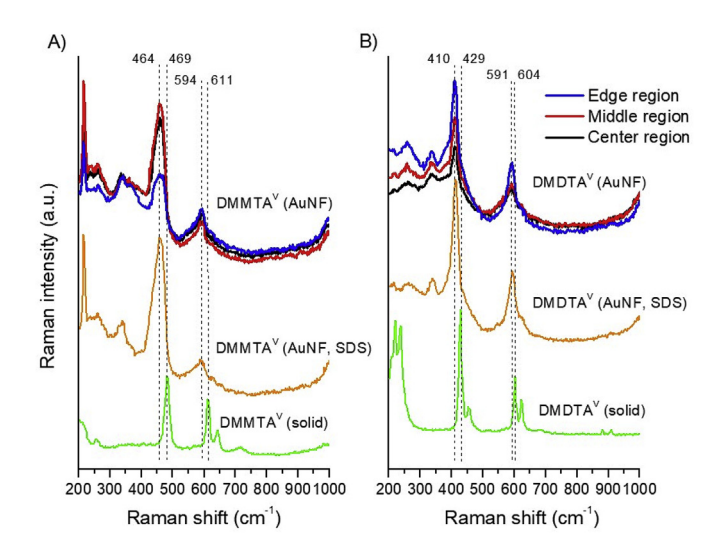


Fig. 4. The SERS spectra of 100 mg L^{-1} A) DMMTA^V and B) DMDTA^V in citrate buffer (pH = 3) onto AuNF during the formation of the coffee ring. For comparison, the standard conditions were achieved by suppressing the coffee ring effect via addition of 0.1% surfactant sodium dodecyl sulfate (SDS).

Separate experiments were repeated multiple times to evaluate the reproducibility of the coffee ringdiameter and the signal intensities of thioarsenicals SERS spectra on different sets of AuNFs (prepared from different batches of AuNPs, but same sizes), and the information was provided in Supporting Information. It was demonstrated that the SERS spectra and signal intensities on different sets of AuNFs were highly reproducible (Table S2, Fig. S3, Table S3).

3.3. Application of the coffee ring effect on AuNF surface for separation and identification of DMMTA V and DMDTA V

As for individual thioarsenicals adsorbed onto AuNF, the mixture of DMMTA^V and DMDTA^V also demonstrated the similar red shift for all vibrational modes (Fig. 5). For DMDTA^V from 429 cm⁻¹ to 412 cm⁻¹ (S–As–S stretching), from 604 cm⁻¹ and 625 cm⁻¹ to 594 cm⁻¹ for As–C symmetric and asymmetric stretching respectively. Regarding DMMTA^V, As=S vibrational frequency shifted from 469 cm⁻¹ to 465 cm⁻¹, As–C from 604 cm⁻¹ to 596 cm⁻¹ respectively. For the separation part, the SERS signal of DMDTA^V increased constantly from center to edge regions, in contrast to the DMMTA^V, which was decreasing across the ring stain. The broad SERS signal at 276 cm⁻¹ was attributed to the Aucitrate vibrational stretching, indicating the presence of citrate coated gold nanoparticles onto the nanofilm surface [55].

4. Discussion

Generally, the coffee ring is created via reducing surface tension of the sessile droplet and enhancing the capillary action generated by closed packing nanoparticles at air, solid and liquid interphase [56]. In a coffee ring phenomenon, a drop of a liquid is placed on AuNF surface, and as the solvent begins evaporating, the liquid is driven to the edge of the evaporating droplet by a radial outward flow (Fig. S5 and Fig. S6, See supporting information).

The key structural element of the developed method is the nanofilm. This functioned not only as a surface for separation, but also as a SERS substrate. Indeed, silica surfaces coated with nanoparticles are among typical SERS substrates and they are usually used only for the amplification of Raman signal [57,58]. However, it is possible to use them as a stationary phase for chromatographic separation because of its strong resemblance to the ion exchange TLC plates. Indeed, the surface of SERS substrate has negative or

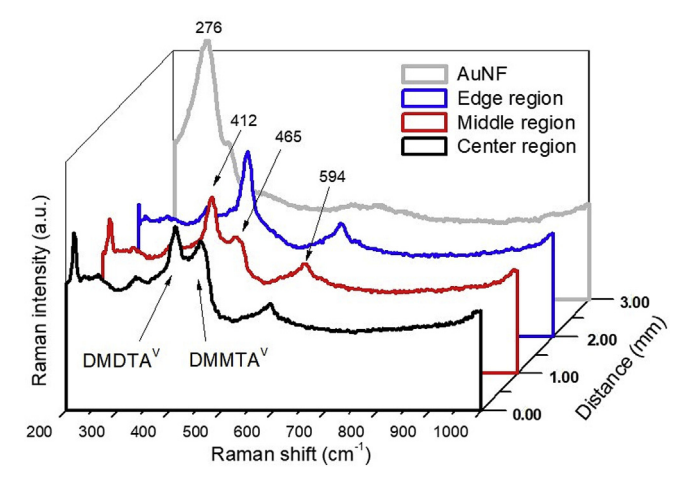


Fig. 5. The coffee ring - SERS spectra of a mixture of 100 mg L^{-1} DMMTA^V and DMDTA^V in citrate buffer (pH=3) onto AuNF. The separation of DMMTA^V and DMDTA^V was obtained during the development of the coffee ring effect.

positive charges depending on the method of preparation of nanoparticles colloidal solution, pKa could influence the charges of thioarsenicals in the buffer solution causing difference in migration distances for each thioarsenical during the formation of the coffee ring. The calculated pKa's for DMMTAV and DMDTAV were 4.37 and 2.25, respectively. According to these results, citrate buffer (pH=3.0) was used to selectively deprotonate the sulfhydryl group of DMDTA^V. Since charged and neutral species would have distinct interactions with negatively charged SERS surface, their travelling distances could be different. It is expected that negatively charged DMDTAV could preferentially stay in the inner ring of the dried droplet because of the strong interaction with AuNF surface in contrast to neutral DMMTAV that has lesser AuNF surface attraction and would be driven by radial outward flow from the center to the edge. The coffee ring effect regions are illustrated in Fig. S6 (See supporting information).

In a previous study [59] we used AgNF to separate four major oxoarsenicals (As^{III}, As^V, MMA^V, DMA^V) based on their distinct pKa's values. The coffee ring effect was evident upon introducing arsenicals onto AgNF surface because the SERS signal intensity of individual species increases from the center to the edge the evaporated droplet. MMAV and DMAV were present across AgNF, in contrast to the As^{III} and As^V that travelled longer distances and were detected in the outer region. This indicates that oxoarsenicals interact with the AgNF surface in a different way, and we attempted to extrapolate this method for the speciation of thioarsenicals, however no SERS signal of arsenic-sulfur bond was found onto AgNF, only DMA^V. It was assumed that AgNPs can catalyze the electron capture by O_2 resulting in the formation of anion of oxygen $({}^2O_2^-)$ [60]. Also, the AgO₂ could be formed under the laser irradiation, oxidizing As-S to As-O onto the AgNF surface. Indeed, the vibrational fingerprint of $Ag^{-2}O_{\overline{2}}$ and AgO_{2} were found onto the AgNF surface. Thus, AgNF was not suitable for easily oxidezible species and we opted for the more inert and biocompatible gold nanofilm (AuNF)

Considering the application of the coffee ring effect for the separation of DMMTAV and DMDTAV, the formation of the coffee ring deposit was influenced by three major factors: the radial outward flow, drawing the thioarsenicals to from the center to the edge of the evaporating droplet; attractive/repulsive interactions between thioarsenicals and AuNF that mainly govern the adsorption of thioarsenicals onto AuNF; and thermally induced Marangoni convection that reverses the solute movement as opposed to the radial flow and promotes the deposition of thioarsenicals in the center region.

The first factor affected the coffee ring deposit formation is the radial outward flow. The construction of a coffee ring stain begins as a droplet placed onto the AuNF and solvent (water) evaporation initiates (Fig. S5). The radial outward flow transfers the liquid to the wetting contact line of the drying drop to replenish solvent that vanishes during evaporation, thus, initially driving both DMMTA^V and DMDTAV out of the center to the edge region. The evaporation velocity is linearly proportional to the height of the evaporating droplet and inversely proportional to the total evaporation time [62]. The height of the droplet, which is radius dependent, accounted for 2.5×10^{-3} m. Total evaporation time of 2 μ L droplet is 30 min, thus the calculated evaporation velocity throughout drying was 5×10^{-2} mg/min (data not shown). Moreover, the radial outward flow is linearly related to evaporating flux [63], and inversely proportional to viscosity of the solution [64]. In previous studies, the radial outward flow considerably affected the separation of particles various sizes [21,65], however in the case of small molecules as an example of thioarsenicals, which size are negligibly small, the radial flow itself is assumed to equally affect their velocities and, thus travelled distances.

The second factor is the attractive/repulsive forces between the thioarsenicals and AuNF that influenced the adsorption of thioarsenicals onto AuNF. As DMMTAV and DMDTAV mixture driven to the edge of the droplet by the radial flow, thioarsenicals begins to interact with the AuNF surface. At pH=3 the AuNF surface displays a negative γ surface potential, because the major surface constituents are H₃Citrate and H₂Citrate that stabilizes the outer laver of AuNPs onto the AuNF surface [66]. It is widely recognizable that thiols and sulfur containing ligands can substitute the citrates onto the nanoparticles surface [67–70]. In addition, pH determines the dissociation of thioarsenicals in the solution, thus leading to the distinct adsorption constants, such as negatively charged thiolates are much more active nanoparticles substituents than neutral thiols, the binding energies of neutral thiols is 3-4 times smaller than that of thiolates [71]. Another factor that must be considered is the effect of the electron density delocalization across arsenic sulfur containing active binding site of thioarsenicals, that may lead to substantial Raman shifts upon adsorption onto AuNF. The importance of this phenomenon was demonstrated upon the aromatic thiols adsorption onto AuNP that exhibits gigantic Raman shifts due to the d-electron transitions [72].

As soon as the mixture was deposited onto AuNF surface, DMDTAV immediately anchors onto AuNF replacing the citrate ligand at the nanofilm surface leading to the remarkable red shift from 429 cm⁻¹ to 412 cm⁻¹ (Fig. 5) for the delocalized π -electrons bond in DMDTAV salt form. Because of the strong attraction between DMDTAV and AuNF, the DMDTAV predominantly occupied the inner region. Exploiting the delocalization effect across S-As-S binding site is the major reason why we intentionally manipulated pH in the way to ionize DMDTA^V, thus in this form of DMDTA^V has substantially higher affinity to the AuNF surface than the neutral DMDTA^V. Even though for the individual DMDTA^V the coffee ring effect was detected: the radial outward flow has driven some of DMDTAV to the edge, in the mixture the DMDTAV's behavior was different, representing its uniform distribution across AuNF. As a result, the SERS signal intensity of DMDTAV was relatively constant from the center to the edge due to its immediate adsorption onto the AuNF surface by substituting citrate that stabilized AuNPs.

In contrast to ionized form of DMDTAV, we selectively left DMMTA^V neutral, consequently, it initially travelled longer distance across drying droplet because it has not been attracted to the AuNF surface as much as DMDTAV, thus facilitating the separation between thioarsenicals. For DMMTAV, the SERS signal intensity at 464 cm⁻¹ (As=S symmetric stretching) was decreasing from the center to the edge indicating that neutrally charged DMMTAV has not been as strongly retained onto the AuNF surface as DMDTAV. As a result, DMMTAV was more affected by the radial flow than DMDTAV, and was driven to the edge region. Considering the interaction between DMMTAV and AuNF, the red shift occurs from 469 cm⁻¹ to 465 cm⁻¹ (Fig. 5) due to the charge transfer effect between its molecule and the AuNF surface [73]. However, in contrast to DMDTAV the SERS shift was significantly smaller, 17 cm⁻¹ for DMDTA^V and 4 cm⁻¹ DMMTA^V (Fig. 5) respectively. This data provides the evidence that DMMTAV has lesser affinity to the AuNF and has not been adsorbed as much as DMDTAV.

The third key factor is the thermo-capillary Marangoni flow that drives the liquid back to the center of the drop [63,74,75]. During the evaporation of the drying droplet, the thermally induced Marangoni flow carries out thioarsenicals back from the edge to the center region, however, DMDTA^V having higher affinity to the AuNF than DMMTA^V, was preferentially deposited in the edge region in contrast to the DMMTA^V, which was transferred back to the center of the evaporating drop. As a result of the predominant repulsion/attraction interaction over radial flow and Marangoni convection, DMDTA^V was deposited uniformly from the center to the edge of

evaporating droplet [64]. Indeed, the temperature profile increases from the center to the edge of the droplet deposited onto the flat surface, meaning that the thermal field gradient in the drop varies considerably as evaporation proceeds [76], might resulting in the reversal direction of Marangoni flow that drives DMMTA^V back from the edge to the center region [63].

Overall, considering all three factors, it can be concluded that outward radial flow initially drives the analytes to the edge of the drying droplet, at that region DMDTAV interacts stronger with the AuNF, considering substantial Raman shift (17 cm⁻¹) in contrast to this of DMMTA^V (4 cm⁻¹) (Fig. 5). Then, thermally-induced Marangoni flow reverses the movement of both analytes affecting deposition of DMMTAV that eventually was detected in the center of the droplet, whereas DMDTAV was anchored gradually across AuNF providing a relatively constant SERS signal of the As÷S stretching at 412 cm⁻¹ (Fig. 5). Additional support for the separation processes associated with the coffee ring effect we analyzed here came from a separate experiment investigating the separation capability of the coffee ring for the mixture of DMAV, DMMTAV and DMDTA^V (Figure S7). For this mixture, DMA^V was found in the edge region of the coffee ring, whereas DMMTAV and DMDTAV were detected in the center and middle regions, respectively. This could be due to the absence of S in DMAV (in comparison to thioarsenicals), which leads to a weaker interaction of DMAV with the AuNF surface and therefore DMAV travelled a longer distance reaching the edge region. This separation could also be pKa-related, as DMAV has a pKa of 6.2 and is mostly neutral at pH=4, thus interacting less strongly with the AuNF surface.

It is worth noting that the migration distances of thioarsenicals under the coffee ring effect-driven separation are relatively short (approximately 3–4 mm vs 100–250 mm usually in HPLC), and the separation efficiency of the coffee ring effect might not be as good as using HPLC. Our intention was to use the distinct fingerprint SERS signals in combination with separation of different thioarsenicals on the SERS substrate plate due to the coffee ring effect for identification of thioarsenicals. This combination would enable the identification of analytes even though the separation might be incomplete, as demonstrated here by the examples of DMMTA^V and DMDTA^V. More studies are warranted to further investigate the separation efficiency of the coffee ring effect and the comparison of this separation method with other conventional methods (e.g., HPLC).

5. Conclusion

The coffee ring effect coupled with SERS is an alternative technique for the separation and identification of thiolated arsenicals. The separation was achieved due to the combination of three mechanisms influencing the formation of the coffee ring deposit: radial outward flow, attraction/repulsion interactions between the AuNF and thioarsenicals and the thermally induced Marangoni flow. The AuNF was employed not only for separation via the coffee ring effect, but also as a substrate for SERS identification. The separation employing the coffee ring effect can be manipulated not only by varying pH that controls the interactions between AuNF and analytes achieving different travel distances, but also by tuning nanoparticles size, droplet volume, and other parameters. Overall, the combination of coffee ring effect and the detection method such as SERS is a promising technique for the speciation of thiolated arsenicals. This work will significantly expand the nanofilm application for speciation analysis concerning speciation of unstable and easily oxidizable species. Separation by the coffee ring effect in mild condition coupled with nondestructive SERS detection method is a powerful tool for the speciation of small molecules.

Declaration of competing interest

The authors declare that they have no known competing financial interests or personal relationships that could have appeared to influence the work reported in this paper.

CRediT authorship contribution statement

Valery Liamtsau: Methodology, Software, Data curation, Writing - original draft. **Changjun Fan:** Data curation. **Guangliang Liu:** Writing - review & editing, Investigation. **Anthony J. McGoron:** Writing - review & editing. **Yong Cai:** Supervision, Conceptualization.

Acknowledgments

The authors gratefully acknowledge NSF programs (ECS1905239 and ECS1710111) for the support of the work. Valery Liamtsau acknowledges the Florida International University for financial support to dissertation research. This is contribution number 943 from the Southeast Environmental Research Center in the Institute of Water & Environment at Florida International University.

Appendix A. Supplementary data

Supplementary data to this article can be found online at https://doi.org/10.1016/j.aca.2020.01.042.

References

- [1] H. Naranmandura, K. Ibata, K.T. Suzuki, Toxicity of dimethylmonothioarsinic acid toward human epidermoid carcinoma A431 cells, Chem. Res. Toxicol. 20 (8) (2007) 1120–1125.
- [2] Q.Q. Wang, D.J. Thomas, H. Naranmandura, Importance of being thiomethylated: formation, fate, and effects of methylated thioarsenicals, Chem. Res. Toxicol. 28 (3) (2015) 281–289.
- [3] C. Fan, et al., Thiolation in arsenic metabolism: a chemical perspective, Metallomics 10 (10) (2018) 1368–1382.
- [4] K. Rehman, H. Naranmandura, Arsenic metabolism and thioarsenicals, Metallomics 4 (9) (2012) 881–892.
- [5] A. Raab, et al., Pentavalent arsenic can bind to biomolecules, Angew. Chem. Int. Ed. 46 (15) (2007) 2594–2597.
- [6] L. Yehiayan, et al., Dimethylarsinothioyl glutathione as a metabolite in human multiple myeloma cell lines upon exposure to darinaparsin, Chem. Res. Toxicol. 27 (5) (2014) 754–764.
- [7] J. Chen, B.P. Rosen, Organoarsenical biotransformations by Shewanella putrefaciens, Environ. Sci. Technol. 50 (15) (2016) 7956–7963.
- [8] R. Raml, et al., Thio-dimethylarsinate is a common metabolite in urine samples from arsenic-exposed women in Bangladesh, Toxicol. Appl. Pharmacol. 222 (3) (2007) 374–380.
- [9] H. Naranmandura, K.T. Suzuki, Formation of dimethylthioarsenicals in red blood cells, Toxicol. Appl. Pharmacol. 227 (3) (2008) 390–399.
- [10] K.M. Kubachka, et al., Exploring the in vitro formation of trimethylarsine sulfide from dimethylthioarsinic acid in anaerobic microflora of mouse cecum using HPLC—ICP-MS and HPLC—ESI-MS, Toxicol. Appl. Pharmacol. 239 (2) (2009) 137—143.
- [11] P. Alava, et al., HPLC-ICP-MS method development to monitor arsenic speciation changes by human gut microbiota, Biomed. Chromatogr. 26 (4) (2012) 524–533.
- [12] B.K. Mandal, et al., A SEC-HPLC-ICP MS hyphenated technique for identification of sulfur-containing arsenic metabolites in biological samples, J. Chromatogr. B 874 (1) (2008) 64–76.
- [13] T. Hayakawa, et al., A new metabolic pathway of arsenite: arsenic-glutathione complexes are substrates for human arsenic methyltransferase Cyt19, Arch. Toxicol. 79 (4) (2005) 183–191.
- [14] S. Ashoka, et al., Comparison of digestion methods for ICP-MS determination of trace elements in fish tissues, Anal. Chim. Acta 653 (2) (2009) 191–199.
- [15] L. Yehiayan, et al., Extraction tool and matrix effects on arsenic speciation analysis in cell lines, Anal. Chim. Acta 699 (2) (2011) 187–192.
- [16] D.S. Dheeman, et al., Pathway of human AS3MT arsenic methylation, Chem. Res. Toxicol. 27 (11) (2014) 1979—1989.
- [17] B. Chen, et al., Arsenic speciation in the blood of arsenite-treated F344 rats, Chem. Res. Toxicol. 26 (6) (2013) 952–962.
- [18] H.R. Hansen, et al., 2-Dimethylarsinothioyl acetic acid identified in a biological sample: the first occurrence of a mammalian arsinothioyl metabolite, Angew.

- Chem. 116 (3) (2004) 341-344.
- [19] J.-Y. Jung, Y.W. Kim, J.Y. Yoo, Behavior of particles in an evaporating didisperse colloid droplet on a hydrophilic surface, Anal. Chem. 81 (19) (2009) 8256–8259.
- [20] W. Wang, et al., Coffee-ring effect-based simultaneous SERS substrate fabrication and analyte enrichment for trace analysis, Nanoscale 6 (16) (2014) 9588–9593
- [21] T.-S. Wong, et al., Nanochromatography driven by the coffee ring effect, Anal. Chem. 83 (6) (2011) 1871–1873.
- [22] J.B. Miller, et al., Phase separation and the 'coffee-ring'effect in polymer-nanocrystal mixtures, Soft Matter 10 (11) (2014) 1665–1675.
- [23] J. Xu, et al., Facile detection of polycyclic aromatic hydrocarbons by a surfaceenhanced Raman scattering sensor based on the Au coffee ring effect, ACS Appl. Mater. Interfaces 6 (9) (2014) 6891–6897.
- [24] M. Yang, et al., Arsenic speciation on silver nanofilms by surface-enhanced Raman spectroscopy, Anal. Chem. 91 (13) (2019) 8280–8288.
- [25] M. Yang, et al., Raman spectra of thiolated arsenicals with biological importance, Talanta 179 (2018) 520–530.
- [26] E.J. Blackie, E.C.L. Ru, P.G. Etchegoin, Single-molecule surface-enhanced Raman spectroscopy of nonresonant molecules, J. Am. Chem. Soc. 131 (40) (2009) 14466–14472.
- [27] E. Le Ru, et al., Surface enhanced Raman scattering enhancement factors: a comprehensive study, J. Phys. Chem. C 111 (37) (2007) 13794–13803.
- [28] M. Osawa, Surface-enhanced infrared absorption, in: Near-field Optics and Surface Plasmon Polaritons, Springer, 2001, pp. 163–187.
- [29] W.R. Cullen, et al., Methylated and thiolated arsenic species for environmental and health research—a review on synthesis and characterization, J. Environ. Sci. 49 (2016) 7–27.
- [30] K.T. Suzuki, et al., Dimethylthioarsenicals as arsenic metabolites and their chemical preparations, Chem. Res. Toxicol. 17 (7) (2004) 914–921.
- [31] M.W. Fricke, et al., Chromatographic separation and identification of products from the reaction of dimethylarsinic acid with hydrogen sulfide, Chem. Res. Toxicol. 18 (12) (2005) 1821–1829.
- [32] G. Schaftenaar, J.H. Noordik, Molden: a pre-and post-processing program for molecular and electronic structures, J. Comput. Aided Mol. Des. 14 (2) (2000) 123–134.
- [33] T. Lu, F. Chen, Multiwfn: a multifunctional wavefunction analyzer, J. Comput. Chem. 33 (5) (2012) 580–592.
- [34] F. Vansant, B. Van der Veken, M. Herman, Vibrational analysis of dimethylarsinic acid, Spectrochim. Acta Mol. Spectros 30 (1) (1974) 69–78.
- [35] T. Watanabe, S. Hirano, Metabolism of arsenic and its toxicological relevance, Arch. Toxicol. 87 (6) (2013) 969–979.
- [36] T.d.A.D.d. Santos, et al., Potentiometric and conductimetric studies of chemical equilibria for pyridoxine hydrochloride in aqueous solutions: simple experimental determination of pKa values and analytical applications to pharmaceutical analysis, Eclét. Quím. 35 (4) (2010) 81–86.
- [37] Y. Dogan Daldal, et al., Liquid chromatographic, spectrophotometric and potentiometric pKa determination of ranitidine and famotidine, Curr. Drug Ther. 9 (4) (2014) 277–284.
- [38] L. Ferrando-Climent, et al., Comprehensive study of ibuprofen and its metabolites in activated sludge batch experiments and aquatic environment, Sci. Total Environ. 438 (2012) 404–413.
- [39] N. Svintsitskaya, et al., A new procedure for synthesis of phosphorylated ynamines, Russ. J. Gen. Chem. 78 (1) (2008) 157–159.
- [40] J.D. McKinney, Metabolism and disposition of inorganic arsenic in laboratory animals and humans, Environ. Geochem. Health 14 (2) (1992) 43–48.
- [41] S.M. Healy, et al., Enzymatic methylation of arsenic compounds: V. arsenite methyltransferase activity in tissues of mice, Toxicol. Appl. Pharmacol. 148 (1) (1998) 65–70.
- [42] P. Lee, D. Meisel, Adsorption and surface-enhanced Raman of dyes on silver and gold sols, J. Phys. Chem. 86 (17) (1982) 3391–3395.
- [43] A.F. Scarpettini, A.V. Bragas, Coverage and aggregation of gold nanoparticles on silanized glasses, Langmuir 26 (20) (2010) 15948–15953.
- [44] M. Fricke, et al., Dimethylthioarsinic anhydride: a standard for arsenic speciation, Anal. Chim. Acta 583 (1) (2007) 78–83.
- [45] I. Haiduc, L. Silaghi-Dumitrescu, Organotin and tin (IV) derivatives of dimethyldithioarsinic acid, J. Organomet. Chem. 225 (1) (1982) 225–232.
- [46] M.W. Wong, Vibrational frequency prediction using density functional theory, Chem. Phys. Lett. 256 (4–5) (1996) 391–399.
- [47] R.A. Zingaro, et al., Rearrangement of tetramethyldiarsine disulfide, J. Am. Chem. Soc. 93 (22) (1971) 5677–5681.
- [48] M. Anyfantakis, et al., Modulation of the coffee-ring effect in particle/

- surfactant mixtures: the importance of particle—interface interactions, Langmuir 31 (14) (2015) 4113—4120.
- [49] H. Hu, R.G. Larson, Marangoni effect reverses coffee-ring depositions, J. Phys. Chem. B 110 (14) (2006) 7090–7094.
- [50] A. Marin, et al., Surfactant-driven flow transitions in evaporating droplets, Soft Matter 12 (5) (2016) 1593–1600.
- [51] C. Seo, et al., Altering the coffee-ring effect by adding a surfactant-like viscous polymer solution, Sci. Rep. 7 (1) (2017) 500.
- [52] P.J. Yunker, et al., Suppression of the coffee-ring effect by shape-dependent capillary interactions, Nature 476 (7360) (2011) 308.
- [53] D.-Y. Wu, et al., Photon-driven charge transfer and photocatalysis of p-aminothiophenol in metal nanogaps: a DFT study of SERS, Chem. Commun. 47 (9) (2011) 2520–2522.
- [54] Y. Su, et al., Quantification and coupling of the electromagnetic and chemical contributions in surface-enhanced Raman scattering, Beilstein J. Nanotechnol. 10 (1) (2019) 549–556.
- [55] S.R. Smith, et al., Characterization of a self-assembled monolayer of 1-Thio-β-d-Glucose with electrochemical surface enhanced Raman spectroscopy using a nanoparticle modified gold electrode, Langmuir 31 (36) (2015) 10076–10086.
- [56] R.D. Deegan, et al., Capillary flow as the cause of ring stains from dried liquid drops, Nature 389 (6653) (1997) 827.
- [57] E. Kočišová, et al., Drop coating deposition of a liposome suspension on surfaces with different wettabilities: "coffee ring" formation and suspension preconcentration, Phys. Chem. Chem. Phys. 19 (1) (2017) 388–393.
- [58] E. Kočišová, M. Procházka, Drop-coating deposition Raman spectroscopy of porphyrins, J. Raman Spectrosc. 46 (2) (2015) 280–282.
- [59] M. Yang, et al., Arsenic speciation on silver nanofilms by surface-enhanced Raman spectroscopy, Anal. Chem. (2019).
- [60] Y.F. Huang, et al., Activation of oxygen on gold and silver nanoparticles assisted by surface plasmon resonances, Angew. Chem. Int. Ed. 53 (9) (2014) 2353—2357
- [61] R. Shukla, et al., Biocompatibility of gold nanoparticles and their endocytotic fate inside the cellular compartment: a microscopic overview, Langmuir 21 (23) (2005) 10644–10654.
- [62] F. Boulogne, F. Ingremeau, H.A. Stone, Coffee-stain growth dynamics on dry and wet surfaces, J. Phys. Condens. Matter 29 (7) (2016), 074001.
- [63] H. Hu, R.G. Larson, Analysis of the effects of Marangoni stresses on the microflow in an evaporating sessile droplet, Langmuir 21 (9) (2005) 3972–3980.
- [64] R. Bhardwaj, et al., Self-assembly of colloidal particles from evaporating droplets: role of DLVO interactions and proposition of a phase diagram, Langmuir 26 (11) (2010) 7833–7842.
- [65] J. Yi, H. Jeong, J. Park, Modulation of nanoparticle separation by initial contact angle in coffee ring effect, Micro. Nano Syst. Lett. 6 (1) (2018) 17.
- [66] J.-W. Park, J.S. Shumaker-Parry, Structural study of citrate layers on gold nanoparticles: role of intermolecular interactions in stabilizing nanoparticles, J. Am. Chem. Soc. 136 (5) (2014) 1907–1921.
- [67] D.A. Giljohann, et al., Gold nanoparticles for biology and medicine, Angew. Chem. Int. Ed. 49 (19) (2010) 3280–3294.
- [68] M.G. Bellino, E.J. Calvo, G. Gordillo, Adsorption kinetics of charged thiols on gold nanoparticles, Phys. Chem. Chem. Phys. 6 (2) (2004) 424–428.
- [69] S.-Y. Lin, et al., Two-step functionalization of neutral and positively charged thiols onto citrate-stabilized Au nanoparticles, J. Phys. Chem. B 108 (7) (2004) 2134–2139.
- [70] G.S. Perera, et al., Facile displacement of citrate residues from gold nanoparticle surfaces, J. Colloid Interface Sci. (2017).
- [71] D. Krüger, et al., Interaction of short-chain alkane thiols and thiolates with small gold clusters: adsorption structures and energetics, J. Chem. Phys. 115 (10) (2001) 4776–4786.
- [72] C. Goldmann, et al., Charge transfer at hybrid interfaces: plasmonics of aromatic thiol-capped gold nanoparticles, ACS Nano 9 (7) (2015) 7572–7582.
- [73] J. Magura, et al., Thiol-modified gold nanoparticles deposited on silica support using dip coating, Appl. Surf. Sci. 315 (2014) 392–399.
- [74] R. Bhardwaj, X. Fang, D. Attinger, Pattern formation during the evaporation of a colloidal nanoliter drop: a numerical and experimental study, New J. Phys. 11 (7) (2009), 075020.
- [75] X. Xu, J. Luo, Marangoni flow in an evaporating water droplet, Appl. Phys. Lett. 91 (12) (2007) 124102.
- [76] X. Zhong, A. Crivoi, F. Duan, Sessile nanofluid droplet drying, Adv. Colloid Interface Sci. 217 (2015) 13–30.